

Shear-Induced Demixing in Polystyrene/Poly(vinyl methyl ether) Blends. 1. Early Stages of Shear-Induced Demixing

H. Gerard and J. S. Higgins*

Department of Chemical Engineering, Imperial College of Science, Technology & Medicine, London SW7 2BY, U.K.

N. Clarke

Manchester Materials Science Centre, UMIST & University of Manchester, Manchester M1 7HS, U.K.

Received October 20, 1998; Revised Manuscript Received April 26, 1999

ABSTRACT: Light scattering has been used to investigate the effect of shear-induced demixing (SID) in polystyrene/poly(vinyl methyl ether) blends of diverse molecular weight distributions down to -30 K below the quiescent spinodal temperature of any blend. The early stage of the demixing process, observed along the vorticity direction, presents features remarkably similar to spinodal decomposition. These include an initial exponential increase of scattered intensity with time and a maximal growth rate for $q = q_m$. This demixing occurs after a shearing time τ_d , which decreases as shear rate increases. The shear-induced demixing process appears to be strongly dependent on the applied shear rate, the experimental temperature, and the polydispersity of the components of the blend. For a given shear rate, this process is faster (higher growth rates and lower τ_d) for blends with a higher polydispersity and for lower experimental temperatures. These results allow quantification of the SID process and give access to data which can test the theories predicting SID by taking into account the effect of stored energy on the thermodynamics or the influence of shear flow on concentration fluctuations.

I. Introduction

The behavior of polymer blends under shear flow is a subject of considerable interest both from a fundamental point of view and from an industrial point of view. An important influence of shear flow on polymer blends is its possible effect on the microscopic and mesoscopic structure of the blends. Two different effects have been observed, depending on shear rate, temperature, and composition. In one range, the homogeneous one-phase region is extended in composition and/or temperature under shear. We call this shear-induced mixing (SIM) but many authors would imply by this term that a phase-separated sample is remixing. Though both phenomena are likely to have a similar origin, we shall call this second effect shear-induced remixing (SIR). In other ranges of temperature and composition, homogeneous one-phase samples become turbid and two phase after shear is applied. We define this as shear-induced demixing (SID). The high shear stresses implied when shearing high molecular weight polymer blends have up to now limited such shear experiments on LCST systems. Those experiments reported have been mainly in a range of temperature for which the blends are demixed under quiescent conditions and this inevitably has led to observation of shear-induced mixing (or remixing) for many polymer blends.^{1–6}

Nevertheless shear-induced demixing (SID) has been observed for a few high molecular weights polymer blends such as polystyrene/poly(vinyl methyl ether) (PS/PVME)^{1,7–11}, poly(ethylene-co-vinyl acetate)/solution chlorinated polyethylene (EVA/SCPE)^{12,13} and poly(styrene-co-maleic anhydride)/poly(methyl methacrylate) (SMA/PMMA)^{14,15} through fluorescence, turbidimetry, light scattering (LS), and/or differential scanning calorimetry (DSC). For PS/PVME blends, one of the most studied polymer blends,¹⁶ presenting a large difference between the rheological properties of the components (T_g for high

molecular weight PVME and PS are respectively around -50 and $+100$ °C), mixing, remixing, or demixing occurs under shear depending on the applied shear and the temperature.^{1,7} Early experiments¹ (heating the sample under shear and observing the shift of the cloud point temperature compared to quiescent experiments) on rather polydisperse blends seemed to imply the appearance of miscibility or immiscibility gaps in agreement with relevant theoretical predictions.¹⁷ These first observations nevertheless did not permit any characterization of the SID process but put the stress on the importance of the rheological difference between each component in this phenomenon. Mechanical improvements of the previous shear apparatus¹² have now enabled us to carry out shear jump experiment below the quiescent spinodal temperature T_{s0} .

In section II of this paper, a short review of theories available to describe spinodal decomposition and shear-induced demixing in polymeric systems is given. The experimental setup and the blends used will be described in the following section. In section IV, results on the enhancement of concentration fluctuations along the vorticity direction are given and will be discussed and compared with relevant predictions in section V.

II. Theoretical Considerations

IIa. Early Stage of Spinodal Decomposition in the Absence of Shear Flow. The modified Cahn–Hilliard theory^{18,19} provides us with a rather simple and usually sufficient description of the spinodal decomposition (SD) process for binary polymeric mixtures. According to this theory, for the early stage of SD one should have for the scattered intensity I

$$I(q, t) = I(q, 0) \exp[2R(q)t] \quad (1)$$

with

$$q = \frac{4\pi n}{\lambda} \sin\left(\frac{\theta}{2}\right)$$

n being the refractive index of the blend, λ the light wavelength, and θ the scattering angle.

The growth rate $R(q)$ can be expressed as²⁰

$$R(q) = q^2 [D_{\text{app}} - 2M\kappa q^2] \quad (2)$$

and M is the diffusional mobility of the system, κ is the coefficient associated with gradient free energy density $\kappa(\nabla\phi)^2$,

$$D_{\text{app}} = -M \frac{\partial^2 \Delta G_m}{\partial^2 \phi} \quad (3)$$

is the apparent diffusion coefficient with ΔG_m being the reduced Gibbs free energy of mixing, and ϕ is the volume fraction of one component in the mixture.

q_m is the fastest growing composition fluctuation wavevector and is constant during the early stage (lasting around $2t_c$) with

$$q_m = \frac{1}{2} \left[- \frac{\partial^2 \Delta G_m}{\partial^2 \phi} / \kappa \right]^{1/2} \quad (4)$$

$$t_c = [q_m^2 D_{\text{app}}]^{-1} \quad (5)$$

and

$$R(q_m) = \frac{1}{8} \frac{M}{\kappa} \left(\frac{\partial^2 \Delta G_m}{\partial^2 \phi} \right)^2 = \frac{1}{2} D_{\text{app}} q_m^2 \quad (6)$$

From eq 1 one can expect to obtain $R(q)$ from a semilogarithmic plot of $I(q, t)$ vs t , and, according to (2), D_{app} from a plot of $R(q)/q^2$ vs q^2 in the region where the mobility term M can be assumed to be independent of q , i.e., for $R_g q < 1$ ²¹ (R_g is the radius of gyration of the polymer molecules), which is the case in our LS experiments.

The description given above applies most of the time to quiescent SD but is not sufficient to describe properly its early stage for systems such as high molecular weight PS/PVME blends.²² In those systems, close to the ones used in this study, $R(q)/q^2$ does not display a linear dependence on q^2 . This deviation from Cahn–Hilliard predictions may be due to the entanglement network and its initial response to deformation.^{22,23} This effect may also be responsible for the long delay times observed, in temperature jump experiments, before the start of SD. Sato and Han²⁴ however claimed that this deviation from Cahn–Hilliard might be due to the thermal noise which is usually neglected. To take this term into account, they proposed to obtain $R(q)$, considering time t such as $R(q)t \ll 1$, from

$$\left[\frac{t}{I(q, t) - I(q, 0)} \right]^{1/3} = \frac{1}{[2(I(q, 0) - I_\infty)R(q)]^{1/3}} \left\{ 1 - \frac{R(q)t}{3} + \frac{[R(q)t]^3}{81} + \dots \right\} \quad (7)$$

where I_∞ is the intensity arising from the thermal noise, including any background intensity for the stray light, and $I(q, 0)$ is the scattered intensity at the time $t = 0$ of the experiment, also including a background intensity.

This approach may solve the nonlinear dependence of $R(q)$ vs q^2 in some cases,²⁴ but the utilization of the experimental time t is a source of problems for systems with apparent delay times, such as high M_w PS/PVME observed in our group²² or even by Sato and Han²⁴ whose results also display a q -dependent delay time. Delay times were also noticed in early works by Bank et al.^{16a} on slightly lower molecular weight PS/PVME blends, but they were associated with the observation of cloudiness by optical microscopy during isothermal experiments. These early results cannot absolutely be compared with those described in our group,²² which should correspond to the onset of the early stage of SD.

In the case of shear flow, some authors²⁵ predict a dependence of $R(q)$ and q_m on the q direction, due to a partial alignment of domains along the flow direction. This approach does not affect the vorticity direction along which our one-dimensional LS experiments have been carried out and just considers a possible deformation of the spinodal structure which develops above T_{s0} in the presence of shear flow.

IIb. Polymer Systems Under Shear Flow. Much theoretical work has been produced to explain the behavior of polymeric solutions under shear,^{26–29} but as in the experimental case, only a few authors have tried to deal with polymer blends. Among them, Horst and Wolf have chosen a purely thermodynamics approach, adding a stored energy term (from Marrucci's dumbbell model³⁰) to the Gibbs free energy of mixing^{17,31} as already proposed for polymer solutions.^{32–33} Qualitatively at least, this can describe the results already available on PS/PVME blends.¹¹ Soontaranun et al.,³⁴ using a similar approach but with a simpler expression for this energy term, were able to predict the phase behavior of SAN/PMMA under shear flow. Both these papers predict SD for values of the shear rate for which the second derivative according to the volume fraction of the modified Gibbs free energy of mixing is negative. For Soontaranun et al.,³⁴ the sign of $\partial^2 \eta(\phi)/\partial^2 \phi$, where $\eta(\phi)$ is the viscosity of the mixed blend for a volume fraction ϕ of one component, is sufficient to predict the behavior of the blend under shear flow: if positive they predict the occurrence of shear-induced mixing, while the condition $\partial^2 \eta(\phi)/\partial^2 \phi < 0$ is necessary but not sufficient to create shear-induced demixing. Chopra et al.³⁵ use a similar approach, with a stored energy term proportional to the first normal stress difference N_1 , itself assumed to have a quadratic dependence on ϕ , and obtain a reasonable agreement with the shear experiments on PS/DOP solutions³² and SMA/PMMA blends.¹⁵

A second possible approach is the main one used for polymer solutions, which attempts to describe the influence of shear flow through a coupling of concentration fluctuations and shear stress,^{27–29,36} which may lead to an enhancement, or a reduction, of these fluctuations. Using the two-fluid model³⁷ and considering that the stress only acts on the "polymer fluid", Ji and Helfand,²⁶ with a simplified Doi–Edwards³⁸ constitutive model to describe the polymer rheological behavior, gave a good description of the concentration fluctuations observed in sheared polymer solutions such as PS in DOP.³⁹ They predict an enhancement of fluctuations along the (1,1) direction in the x, y plane and a "butterfly pattern", with a "dark streak" along z in the x, z plane, as was observed experimentally.

Clarke and McLeish⁴⁰ use the two-fluid model, as in Doi and Onuki,⁴¹ now considering both "fluids" to be

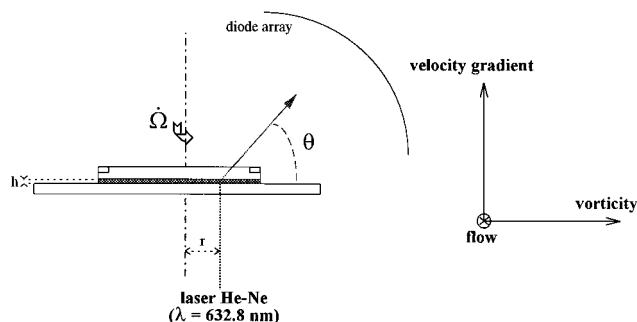


Figure 1. Experimental setup of 1D light scattering experiment.

viscoelastic which introduces, for the simple constitutive models, two relaxation times and two plateau shear moduli. The competition between each component to lower its stresses is ruled by these rheological properties and is predicted to lead to diverse results, according to the mismatch of respective relaxation times and shear moduli. In the vorticity direction, at a given temperature and for a given composition, this theory predicts⁴⁰ a growth rate (analogous to that of the Cahn–Hilliard theory) of

$$R(q_z) = -q_z^2 D_{\text{eff}}(q_z) = q_z^2 [D_{\text{app}0} - 2M\kappa q^2 - A\dot{\gamma}^2] = q_z^2 [D_{\text{app}}(\dot{\gamma}) - 2M\kappa q^2] \quad (8)$$

where $D_{\text{app}0}$ is the temperature- and composition-dependent apparent diffusion coefficient in the absence of shear flow and $A\dot{\gamma}^2$ the shear flow contribution to this diffusion coefficient explicitly described in the Appendix. One must notice that these equations are limited to the weak shear regime, i.e., for $\dot{\gamma}\tau < 1$, where τ is the longest relaxation time in the blend.

Indeed, this description, as most of the other modified Cahn–Hilliard theories, predicts a linear dependence of $R(q)/q^2$ in q^2 , which we know not to be verified, at least when using the classical $\ln(I(q, \theta))$ vs q approach to extract $R(q)$, for quiescent spinodal decomposition for high M_w PS/PVME blends.

III. Experimental Work

IIIa. LS Experiments Under Shear Flow. One-dimensional LS experiments have been carried out with a laboratory-built apparatus described earlier¹² whose mechanical setup (motor and upper plate rotation system) have been improved to provide us with a wider range of observable shear rates. This apparatus allows us to release and quench the samples quickly (i.e., in less than 15 s) once the shear stops. The diode array (consisting of two parallel rows of diodes) collecting the scattered light over an angular range of 60° was set along the vorticity direction (see Figure 1). The fact that our array consists of two parallel rows implies that at least one of these will be parallel to the vorticity direction but slightly shifted (about 4°) along the flow direction.

The shear flow results from the rotation of the upper glass slide of the sample, corresponding to the shear flow imposed during “parallel plate” rheological experiments. The shear rates given in our results are calculated using

$$\dot{\gamma} = \Omega r/h \quad (9)$$

where Ω is the angular velocity of the upper plate, r is the radius at which the observation is carried out, and h is the sample thickness. This basic expression indeed implies a no-slip assumption which might not be correct for the highest observed shear rates.

Table 1. Characteristics of the Blends Used

	M_w (kg/mol)	M_w/M_n	T_g (°C)	70/30% w/w blend T_g (°C)	70/30% w/w blend quiescent spinodal temp (T_{s0}) (°C)
PVME	89	2.5	−32		
PS1	270	4.7	106.6	−15.5 ± 4.	101.8 ± 0.5
PS2	310	4.1	107.2	−15.9 ± 3.	103. ± 0.4
PS3	283	1.35	108.7	−19.4 ± 0.5	101.5 ± 0.4

It should be noted that normal forces arising when shearing such viscoelastic materials are not compensated by pressure on the plates as in a conventional rheometer and lead to an increase of the sample thickness h (up to 10%) during the experiment. All $\dot{\gamma}$ quoted in the following sections correspond to the initial shear rate calculated with the initial thickness.

IIIb. Materials. Three 30/70% w/w PS/PVME blends have been investigated. This composition is close to the critical values for such blends.^{7,16c} The same PVME was blended with three different PS, two “industrial” samples and a monodisperse one. The polymers and blends characteristics are given in Table 1, the molecular weight moments of each component being determined using gel permeation chromatography (the PVME weights are in PS equivalents). All blends were prepared by solution casting (15% w/w in toluene) and then dried for 1 month (6–8 h at room temperature and pressure and then put in a vacuum oven increasing temperature up to 55 °C and reaching full vacuum after 1 week). After 1 month of such drying, the sample weights have reached an asymptotic value, confirming that the blend is mostly solvent-free though some negligible amount of solvent might still be trapped in the blend. The dry samples have a thickness between 70 and 150 μm .

The samples prepared for one-dimensional light scattering shear experiments were then kept a further month under the same conditions to obtain a good contact with the upper (rotating) glass slide.

IIIc. Determination of T_g and T_{s0} . The quiescent spinodal temperatures T_{s0} displayed in Table 1 have been determined through heating ramp and temperature jump 1D LS experiments. These ones enable us to obtain parameters such as D_{app} , q_m and R_m , which should become zero at $T = T_{s0}$.¹⁸ The extrapolation of their values to zero gives an estimation of this quiescent spinodal temperature T_{s0} . However $R(q)/q^2$ does not display linear dependence on q^2 over the whole accessible q range, as already observed for high molecular weight PS/PVME blends.²²

The glass transition temperatures T_g were obtained by DSC measurements on a Perkin-Elmer Pyris 1 with a heating rate of 20 °C/min. The values correspond to the inflection point of the DSC traces, the uncertainty given corresponding to the uncertainty due to the width of the transition averaged for at least three DSC experiments. The uncertainty in T_{s0} corresponds to that in the experimental temperature (± 0.2 °C) plus that arising from the estimation of the spinodal temperature.

IIId. Scattering Experiments under Shear. All shearing experiments were carried out at a constant temperature T lower than T_{s0} . A shear jump was achieved at $t_s = 0$ after the sample had been kept 1 h at T to ensure initial thermal equilibrium.

IV. Results

IVa. General Features of Shear-Induced Demixing. One-dimensional LS experiments were carried out for $-30\text{K} < \Delta T < -7\text{K}$ ($\Delta T = T - T_{s0}$) and $\dot{\gamma}$ between 0.7 and 50 s^{-1} . For any observed shear rate the scattered intensity at a given wavevector \mathbf{q} , initially constant or slightly decreasing with time, starts increasing exponentially (following $I(\mathbf{q}, t) = I(\mathbf{q}, t_d) \exp(2R(\mathbf{q})(t - t_d))$) after a time t_d depending on \mathbf{q} (see Figure 2). During this “early stage” $R(q_z)$ presents a maximal value for a wavevector q_m in the q_z range corresponding to the minimal value plateau displayed by $t_d(q_z)$ (see Figure

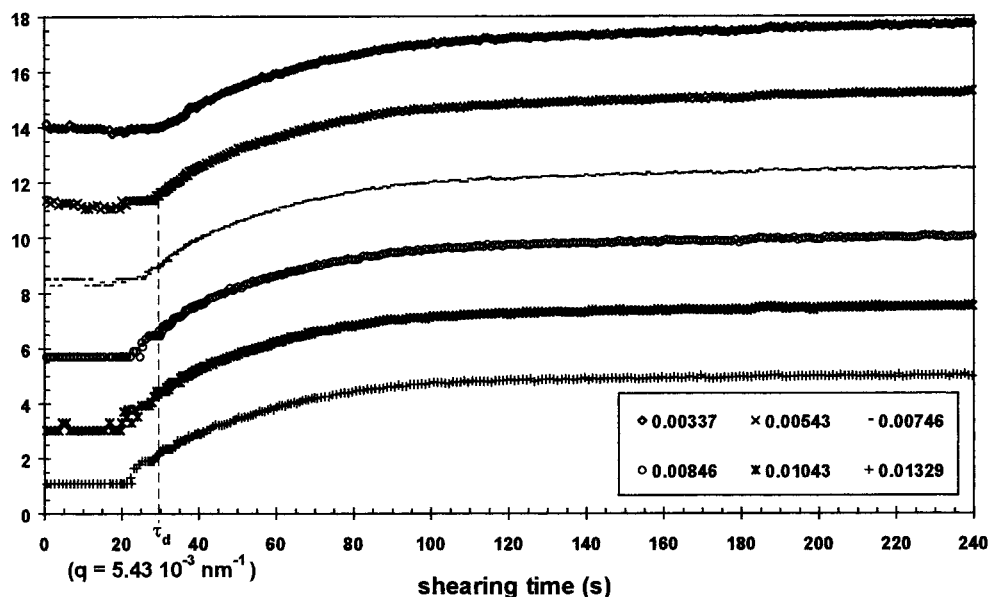


Figure 2. Blend 2, $\dot{\gamma} = 6.5 \text{ s}^{-1}$ at $\Delta T = -11.3 \text{ K}$: scattered intensity according to shear time for different wavevectors \mathbf{q} (in nm^{-1}). Intensities are shifted to allow an easy reading.

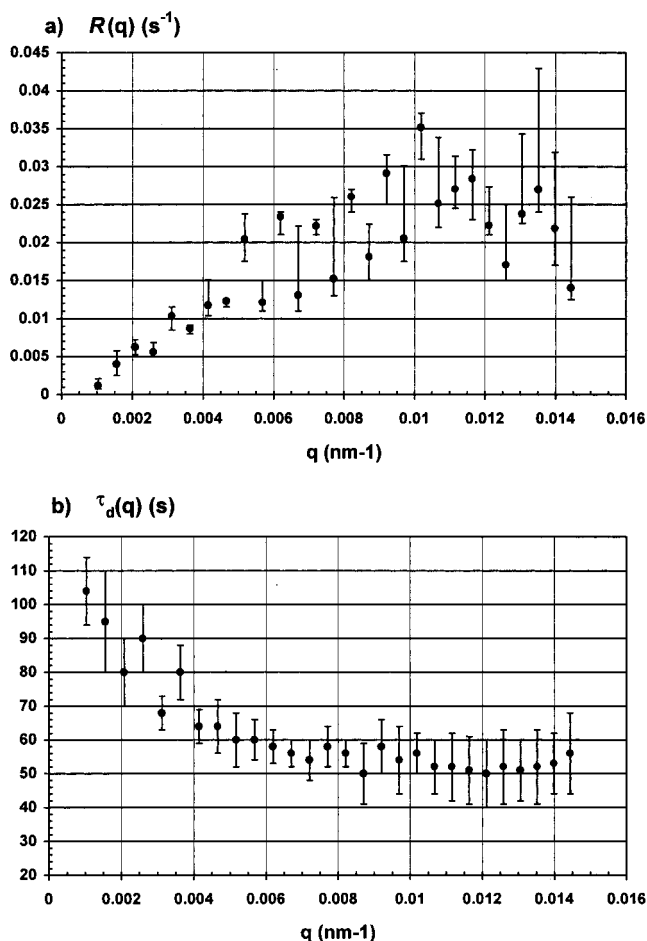


Figure 3. (a) $R(q)$ of blend 2 sheared with $\dot{\gamma} = 2.6 \text{ s}^{-1}$ at $\Delta T = -5.1 \text{ K}$. (b) $\tau_d(q)$ for the same experiment.

3). Such an exponential growth of scattered intensities was already observed for the EVA/SCPE blend¹³ but the $R(q_z)$ did not display any maximum in this case, a feature possibly due to the q range limitation of the experiment. One must also note the anisotropy of the scattered intensity, the intensities observed along the vorticity direction \mathbf{z} being inferior to the ones observed

on the second diode row, corresponding to \mathbf{q} with a component along the flow direction. This anisotropy may also be observed in the $R(\mathbf{q})$ and $\tau_d(\mathbf{q})$ values, τ_d values being generally larger for wavevectors along \mathbf{z} than those observed for wavevectors with a component along \mathbf{x} .

After this “early stage” the intensity continues to increase in an “intermediate stage” with far lower growth rates. The highest growth rate tends toward lower q values (see Figure 2).

After this “intermediate stage” has been reached both sheared samples display a central optically clear circle surrounded (for $r > r_0$, or $\dot{\gamma} > \dot{\gamma}_0$ from eq 9) by a cloudy halo, as already observed in earlier experiments.^{1,8}

IVb. Early Stages of Shear-Induced Demixing. Assuming that the observed demixing is a spinodal process following Cahn–Hilliard theory, one can access the apparent diffusion coefficient D_{app} which should be equal to $(R(q)/q^2)_{q \rightarrow 0}$. However for our PS/PVME blends, as in some quiescent experiments, $R(q)/q^2$ does not display linear dependence on q^2 . This may be due to the fact that we may consider “intermediate” stage data rather than the “early stage” ones due to the limitation in the q range and the relatively bad statistics for the high q range. As already mentioned, the method proposed by Sato and Han²⁴ (eq 7) cannot be applied straightforwardly in our case because of the existence of a q -dependent delay time τ_d though thermal noise may explain this kind of behavior, as does the consideration of entanglement lifetime for high molecular weight polymer blends²² (a third possibility for the cause of this behavior is briefly discussed toward the end of section V). The difficulty in extracting D_{app} therefore lies in the choice of the q range to be considered. Another problem is the low intensity observed at high angles which implies increasing error bars on the values extracted for both delay time and growth rate $R(q)$. This is why we present here the initial observed maximal growth rate R_m (see Figure 4) which should be equal to $R(q_m)$ but which might be underestimated due to the limitation of our q range ($0.001\text{--}0.015 \text{ nm}^{-1}$). One must note that the uncertainty in $\dot{\gamma}$ values can reach 10%, due to the error in the sample thickness measurement.

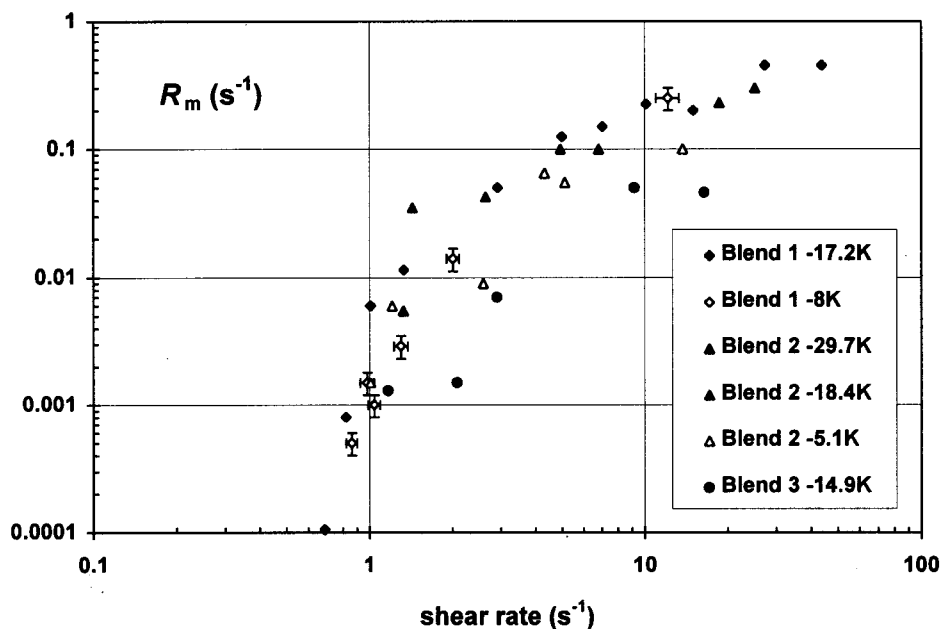


Figure 4. Observed R_m according to shear rate for different blends and ΔT . The error bars displayed for blend 1 data at $\Delta T = -8$ K apply to all data.

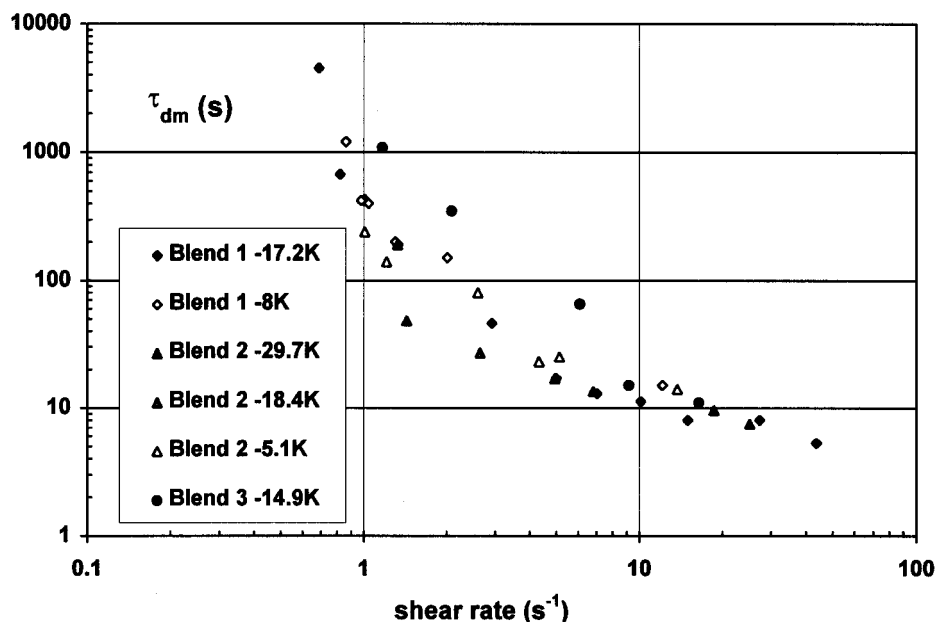


Figure 5. Minimal observed delay time τ_{dm} for different blends and ΔT .

The sharp decrease in R_m observed for shear rates below 1 s^{-1} should correspond to Weissenberg numbers < 1 , according to results obtained for monodisperse PS/PVME blends by Kapnistos et al.,⁴² a value below which the molecule has enough time to relax and is not affected by the shear strain. For such low shear rates the contribution of stored energy to the modified Gibbs free energy should become negligible. This shear rate threshold around 1 s^{-1} was already observed by Katsaros et al.⁸ for a similar blend in the same range of temperatures.

The observed $q_m(\dot{\gamma})$ exhibits the same behavior as R_m , reaching values above 0.015 nm^{-1} for shear rates higher than 1 s^{-1} , though here again, the low intensities observed for high q and our limited q range limit our investigation and make uneasy the estimation of this possible q_m .

The minimal observed delay time τ_{dm} , corresponding to $\tau_d(q_m)$, displays a behavior which follows the observed maximal growth rate (see Figure 5), higher delay times corresponding to lower growth rates and shear rates for both blends and both experimental temperatures.

When comparing results in Figures 4 and 5 for different values of ΔT for each polydisperse blend (1 and 2), at lower temperature or further away from T_{s0} , there is a tendency for the demixing process to become faster, which is consistent with the possible "immiscibility island" predicted by Wolf and Horst.¹⁷ This might be an indication that a better parameter to consider would be the shear stress rather than the shear rate, a given shear rate at low temperature, implying shear stresses higher than those at higher temperatures. It is also noticeable that the shear-induced process seems rather

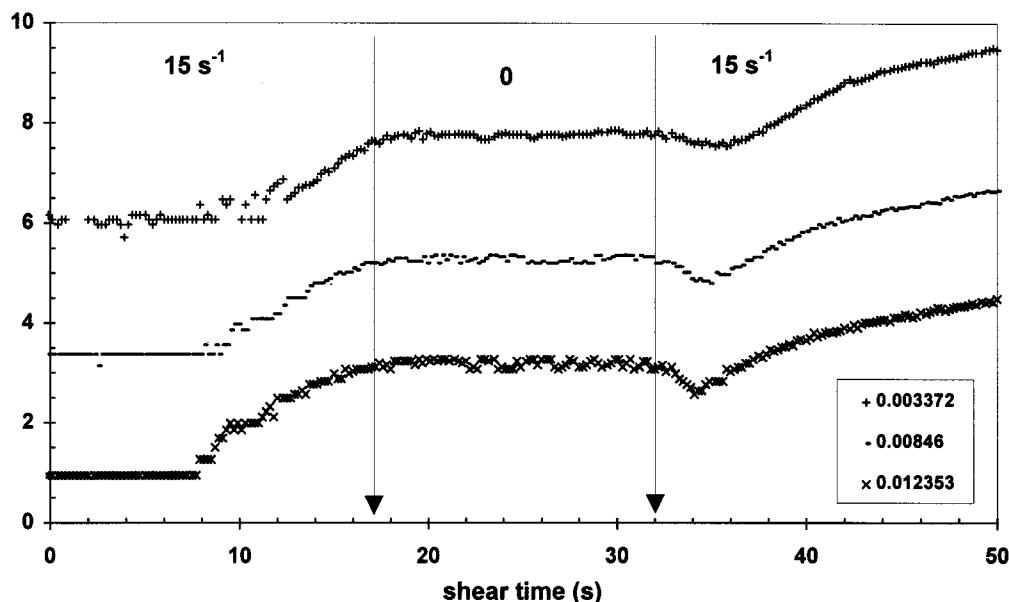


Figure 6. Double shear jump experiment scattered intensity. Blend 1, $\Delta T = -17.2$ K.

slower in the monodisperse blend than in polydisperse ones. Polydispersity will have an influence both on the Gibbs free energy and also smaller molecules (polymeric or additives) will act as lubricants.

IVc. Stability of the Shear-Induced Demixed State. The question of stability of the structure developed under shear flow once the shearing stops is an important one for at least two reasons. The first is its practical importance for industrial processing; the second is the ability to carry out further experiments on a quenched sheared sample. To quench a sample after cessation of shear flow takes a maximum of 15 s. To investigate the possible influence of this time on any final structure, a double shear jump experiment was performed during which the sample is sheared until it starts demixing, and then the shearing is stopped for 15 s after which a second shear jump (at the same shear rate) is carried out. The scattered intensities observed during this experiment are displayed in Figure 6.

The constancy of the scattered light intensity after the cessation of shear in the double shear jump experiment not only confirms that quenching a sheared sample in about 15 s seems sufficient to preserve its shear-induced structure (on a LS scale at least), as was already observed by Mani et al.,⁹ but also sheds light on the influence of strain history on the system response to a shear jump. The most striking feature is the fact that, after the shear flow is stopped before the end of the "early stage", the scattered intensities decrease with significant rates during the second shear jump and then increase again with similar rates (in absolute values). The values are in the same range as these during the early stages after the first jump but are now instead q independent (see Figure 6). This behavior, sometimes observed for the first shear jump, is reminiscent of the results of Werner et al.¹⁰ where they observed while shearing below the quiescent spinodal decomposition temperature an initial shrinking of the scattering 2D LS pattern followed by a "butterfly pattern" development.

An initial decrease of scattered intensities may also be observed after a first shear jump. A possible explanation for this behavior is the initial networklike response of a highly entangled system to the strain,²² which

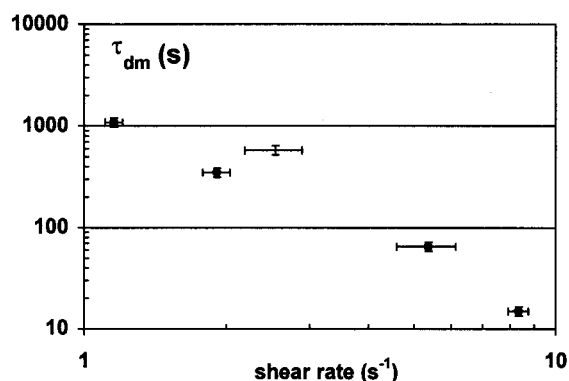


Figure 7. Effect of predemixing on shear-induced demixing kinetics, $\tau_{dm}(\dot{\gamma})$, for blend 3, $\Delta T = -14.9$ K for "equilibrium" samples (circle) and "predemixed" ones (cross).

might also explain the nonlinear dependence of $R(q)$ on q^2 . Our polymers are well entangled ($M_{ePS} = 18\,000$,⁴³ $M_{ePVME} = 6000$ ⁴²), but in our double shear jump experiment, the first jump does not lead to such behavior. This particular feature might nevertheless be considered as resulting from the initial response of a preexisting structure, either a partially demixed one or an entanglement network.

IVd. Influence of Nonequilibrium Conditions on the Shear-Induced Demixing Process. All the results given above arise from experiments in which the sample is raised from 55 °C to the experimental temperature and held at this temperature for at least 1 h before starting the shear (except in the double shear jump experiment). These experiments provided us with kinetic parameters (τ_{dm} and R_m) with a clear trend with respect to $\dot{\gamma}$. The question now arises as to whether for a shear jump experiment with a sample whose "history" is somehow different, the kinetic results obtained may also be quite different.

In Figure 7 are the results obtained for a sample which was demixed for 2 h at $\Delta T = 2$ K and then kept at the experimental temperature for a further 2 h before starting the usual experimental procedure. After 2 h at $\Delta T = -14.9$ K, the sample seemed optically remixed. The huge difference found in kinetics parameters of SID

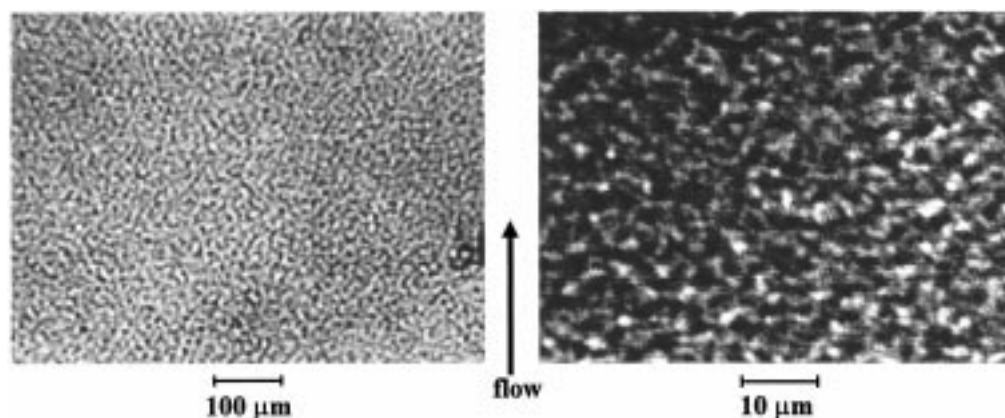


Figure 8. Optical micrograph of the bulk of a blend 2 quenched sample after 25 min shear at $\Delta T = -18.4$ K and $\dot{\gamma} = 2$ s $^{-1}$ for two different magnifications.

for this sample indicates that 2 h were not sufficient for a proper remixing of the sample. Starting from this nonequilibrium state, the process of SID might correspond to that observed for higher temperatures assuming this blend follows the same trend that the more polydisperse ones (i.e., the higher the experimental temperature, the slower the process).

These results, together with the ones reported above, stress the influence of the thermal and strain history of a blend on its reaction to shear flow. Both of these equilibrium perturbations, either thermal or mechanical, have enough influence to affect the structure of the polymeric system (through concentration fluctuations enhancement or attenuation) which will be then affect the initial response of the system to shear flow.

Ive. Optical Microscopy. Microscopy of sheared samples quenched in the “intermediate” stage display SD-like patterns in the bulk with no clear sign of the anisotropy (see Figure 8) reported by optical microscopy in previous literature.^{44,45} It is noticeable that the size of the observed domains is always of the order of a few micrometers for all the samples observed shortly after the attenuation of the initial sharp increase of scattered intensity. “Early stage” smaller domains which, according to our results on the kinetics of shear-induced demixing, should be present for lower shear rates (closer to the center of our sample) are undetected by microscopy. This is due to the fact that the relative compositions of these early domains are too close to be able to distinguish them and also to their very small characteristic sizes in the early stage (below 400 nm for the shear rate ≥ 1 s $^{-1}$).

These microscopic observations present similar features to those recently reported for a PI/PB blend⁴⁶ under shear for $\Delta T > 0$. Optical microscopy of quenched sheared samples which had reached the “intermediate stage” of SID enable us to observe domains of a few micrometers with no clear sign of anisotropy. Up to now, no experiment has enabled us to observe domain characteristic sizes higher than 20 μ m. This may be due to the fact that, above a threshold strain, because normal forces are not compensated for during our experiments, the sample tends to slip from the edges of the upper rotating plate, enabling air layers to get between and then to migrate toward the center of the sample. This perturbation usually reaches the laser beam after the sample has entered the “intermediate stage” at which point the experiment has to be stopped. The limitation of our observed domain sizes might also,

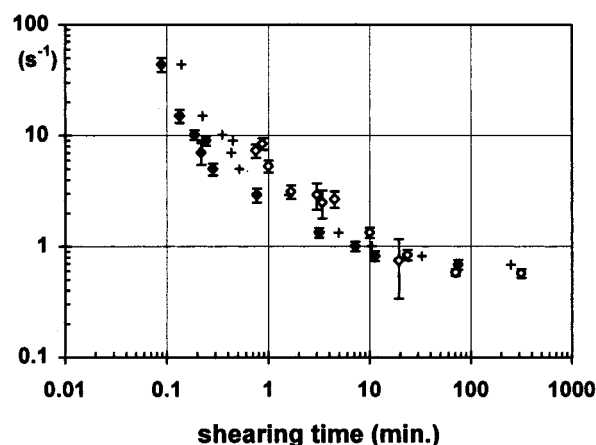


Figure 9. Minimal shear rates $\dot{\gamma}_0$ (open diamonds), $\dot{\gamma}_e$ (filled diamonds), and $\dot{\gamma}_i$ (crosses) for blend 1 at $\Delta T = -17.2$ K. The uncertainty on shearing times are ± 1 s for $\dot{\gamma}_0$ and $\pm 10\%$ for the other minimal shear rates.

however, be due to the phenomenon of shear droplet breakup.^{47–49} That the domain sizes observed through microscopy are rather large compared with the initial observed q_m values confirm the existence of a coarsening process during SID as might already be guessed from LS experiments, where q_m tends toward lower values once entering the “intermediate stage”.

Several “critical” values of the shear rate might be extracted from these experiments. In Figure 9 we compare three of them, $\dot{\gamma}_0$, $\dot{\gamma}_e$, and $\dot{\gamma}_i$, for the blend 1 at $\Delta T = -17.2$ K.

$\dot{\gamma}_0$ is the minimal shear rate to observe optically demixing after a given shearing time.

$\dot{\gamma}_e$ is the minimal shear rate to observe the early stages of SID in a LS experiment after a given shearing time. Since τ_{dm} increases when $\dot{\gamma}$ decreases and no sign of demixing is apparent, for any value of shearing time t_s , for $\dot{\gamma} < \dot{\gamma}_0$, we take $\dot{\gamma}_e = \dot{\gamma}$ for $t_s = \tau_{dm}(\dot{\gamma})$.

$\dot{\gamma}_i$ is the minimal shear rate needed to reach the “intermediate stage” of SID for a given shearing time t_s . $\dot{\gamma}_i$ may be estimated from $\dot{\gamma}_i(\tau_{dm} + 2t_s) = \dot{\gamma}_e(\tau_{dm})$, t_s being calculated (or (over-)estimated for high shear rates) by eq 5.

From Figure 9 it is noticeable that $\dot{\gamma}_0 > \dot{\gamma}_e$, which seems natural since $\dot{\gamma}_0$ should correspond to a later “intermediate stage” for which one can optically observe domains of different compositions and should be compared with the minimal shear rate enabling the sample to reach this “intermediate stage”, $\dot{\gamma}_i$. From Figure 9 it

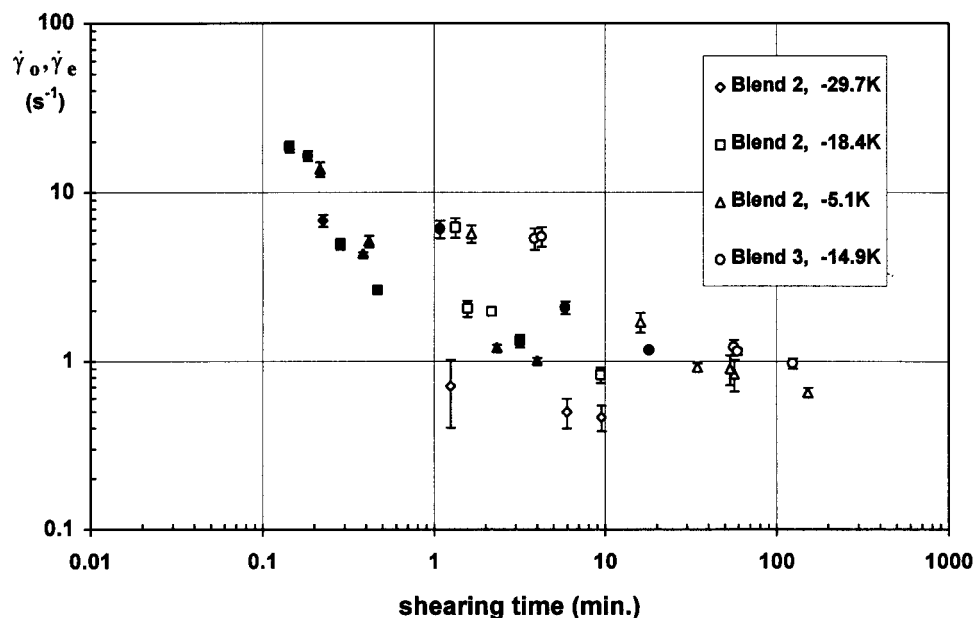


Figure 10. Minimal shear rates $\dot{\gamma}_o$ (open symbols) and $\dot{\gamma}_e$ (filled symbols) for blends 2 and 3.

is also clear that $\dot{\gamma}_o \approx \dot{\gamma}_i$, confirming that the optical observation of SID corresponds to an intermediate stage. In Figure 10 one can see that the lower the temperature, the lower the time needed to observe (either optically or through LS) demixing at a given shear rate. This tends to support a shear stress rather than a shear rate approach.

V. Discussion

Our results partially confirm earlier observations^{1,7} which were consistent with the immiscibility island predicted by Horst and Wolf.¹⁷ The only results from Fernandez et al.⁷ we can compare with the current data are those from the "monodisperse" blend PS1/PVME of this paper whose characteristics are close to those of our blend 3. The results given in this previous paper are normalized as $\Delta T_c(\dot{\gamma})/T_{c0}$, where T_{c0} is the quiescent cloud point and ΔT_c its shift under shear, both obtained through turbidimetry measurements with a heating rate of 1°C min^{-1} . The decrease of this normalized shift when $\dot{\gamma}$ increases is perfectly consistent with our results which show that the lower the shear rate, the higher the delay time and so, in a heating ramp experiment, the higher the observed cloud point temperature. However, for $\dot{\gamma} > 5 \text{ s}^{-1}$ an increase of $\Delta T_c(\dot{\gamma})/T_{c0}$ was also observed,^{1,7} explained by none of our kinetics results.

The "spinodal-like" demixing process observed with our PS/PVME blends was not observed, except for the initial exponential growth of scattered intensities, in the EVA/SCPE case,¹³ which the authors claimed might be due to the fact that a possible q_m might be out of the observed q range for their blend. They neither observed, nor mentioned, the existence of a delay time but their investigation involved only a limited range of temperatures (a few degrees around T_{s0}) and only one shear rate.

The comparison of results obtained for our three different blends indicates the importance of polydispersity in the SID process, which is not surprising since polydispersity may have a very large effect both on thermodynamics and rheology of polymer systems. This effect is best seen in Figure 10 where the "optical" delay time for a given shear rate is far higher for a (relatively)

monodisperse blend than in an equivalent more polydisperse one.

Comparison of our results with relevant theoretical predictions is not an easy task for the thermodynamical approach^{17,31,34,35} since this approach would require the knowledge of the blend rheology for a large number of compositions for each experimental temperature. This investigation of the rheological properties of the blend according to composition is moreover limited by the fact that our experiments are carried out below the glass transition temperature of blends with a high PS content. For the Clarke and McLeish⁴⁰ approach, we also require values for two relaxation times and two moduli for each temperature and their dependences according to composition (see Appendix). A quicker test can be made thanks to eq 8 which predicts a linear dependence of $D_{app}(\dot{\gamma})$ on $\dot{\gamma}^2$. We have seen that this approach cannot properly describe the dependence of the growth $R(q)$ on q and are once again confronted by the problem of which experimental D_{app} to choose to compare with that given by eq 8 (since, according to our results, the derivative of $R(q)/q^2$ with respect to q^2 is q dependent). We have chosen the convention of extracting D_{app} from $R(q)$ values for $q > q_m$ or, when q_m is out of range, $q > 0.01 \text{ nm}^{-1}$. The resulting values for D_{app} are displayed in Figure 11 along with the fits according to eq 8 with fitting parameters D_{app0} and A given in Table 2.

The fits according to eq 8 are very good for the lowest observed shear rates, i.e., for the weak shear regime described in ref 40, though one must keep in mind the uncertainty in the values of D_{app} due to its problematic extraction. The values obtained for D_{app0} correspond, in absolute value, to those found for quenches inside the quiescent spinodal for $\Delta T = 1.5\text{--}5 \text{ K}$ (see Table 2) and are not unlikely if one considers eq 3. They result from combination of a thermodynamical term, whose absolute value may be far higher than for such a small positive ΔT inside the quiescent spinodal with a mobility term whose value will decrease sharply at these much lower temperatures. For the same reason, the variation of D_{app} with ΔT seems reasonable, implying the overwhelming importance of the temperature variation of the thermodynamic term. A is a factor depending mainly on the

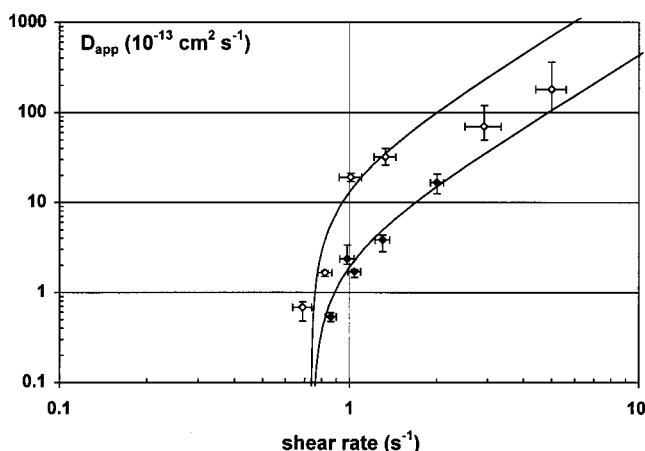


Figure 11. Dependence of D_{app} on $\dot{\gamma}$ for blend 1 at $\Delta T = -17.2$ K (open symbols) and -8 K (filled symbols) and Clarke and McLeish predictions⁴⁰ (lines) with parameters given in Table 2.

Table 2. Values of Apparent Diffusion Coefficient and Parameter A of Blend 1 for SID and Quiescent SD

ΔT (K)	D_{app0} (10^{-13} cm ² s ⁻¹)	A (10^{-13} cm ² s)
-17.2	-15 ± 5.5^a	-28.5 ± 7
-8	-2.4 ± 1.0^a	-4.3 ± 1.1
+1.2	1.2 ± 0.2^b	
+4	4.5 ± 0.6^b	

^a Fit according to eq 8. ^b From temperature jump into the spinodal.

mismatch of rheological properties of the components (see Appendix). Estimating its value is once again a difficult task since it requires the knowledge of the behavior of relaxation times according to composition.

The main drive in the SID process for our PS/PVME blends, if one still follows the Clarke and McLeish approach,⁴⁰ is the value of the dimensionless parameter α (see Appendix) which is highly dependent on the composition and molecular weights of each component. If one follows this approach, one can see that, since we observe SID for our molecular weights, this effect would be canceled and then reversed (i.e., SIM) for higher PS M_w (or lower PVME M_w).

The values obtained from eq 8 now need to be compared with experimental ones. D_{app0} should be obtainable through LS quench experiments (keeping in mind the possibility of delay times occurring during such experiments and a probable nonlinearity of $R(q)/q^2$ vs q^2). A quick check may be done thanks to our double shear jump experiments for which we have seen that the intensity detected after stopping the shear stay stable over our whole q range for 15 s. We find a D_{app0} of -1.5×10^{-12} cm² s⁻¹ from eq 8 for this experimental temperature which gives us, for our highest q value, a minimal growth rate of about -0.035 s⁻¹, and this cannot explain the time behavior observed in Figure 6. This observation may have two origins: either the value of the apparent diffusion coefficient obtained through eq 8 is unrealistic, or a delay time exists before remixing occurs. The first implies either the inadequacy of the Clarke and McLeish approach or the need to take into account the influence of molecular deformation^{31,50} on the thermodynamics of the system (i.e., use a strain-dependent D_{app0} possibly related to a strain-dependent T_g). The possibility of a delay time may arise from the fact that diffusion rates in and from the domains is likely to be limited for the high PS content ones whose

T_g is closer to the experimental temperature¹² though the fact that this remixing occurs in the "early stage" where concentration gradient and domain sizes are still limited appears to eliminate such an explanation. Another problem is due to the fact that, within the adiabatic approximation, it is assumed that the dynamic time scale associated with concentration fluctuations is much slower than that of stress relaxation, i.e., that $D_{app}q^2 < 1/\tau$. Hence, for high enough shear rates (here, ≥ 1 s⁻¹), the adiabatic approximation used is unlikely to hold due to the fact that $D_{app}q^2 > 1/\tau$ for these experiments. It is worth mentioning here that this nonadiabatic behavior is also a potential source of the $R(q)/q^2$ curvature discussed earlier. Rheological experiments are needed to confirm the estimation of A and verify the value of the Weissenberg number for our threshold shear rates. The results of such experiments will be analyzed in a future paper.

The origin of the delay time observed during our experiments is still not absolutely clear, but at least two major contributions may be considered. The first and most obvious one is the time needed to achieve a steady shear flow, or build up a sufficient shear stress, comparable to the time needed for the system to store its elastic energy. In the Appendix, an early attempt is made to express the time needed to reach this rheological steady state. The other contribution is the delay time observed in quiescent spinodal systems on similar blends.²² This last contribution, which has up to now been scarcely observed, may be inherent to the quiescent SD process but difficult to detect for most polymeric systems which show higher "mobility" than the very high molecular weight samples for which it was reported.²² The simple approach used in the Appendix does not yet permit us to draw firm conclusions about the observed delay times reported here for the weak shear regime. However, it does confirm that the building of shear stress and its derivative with respect to composition make an important contribution to this phenomenon.

VI. Conclusion

Shear-induced demixing has been observed in three PS/PVME blends of different polydispersities for ΔT from -5 to -30 K and shear rates between 0.7 and 40 s⁻¹. Following a shear jump from a thermal equilibrium state (i.e., in our case, a mixed sample with small vanishingly concentration fluctuations), scattered intensities along the vorticity direction z start increasing exponentially after remaining initially constant or even slightly decreasing. The increase, with an initial growth rate $2R$, starts after a delay time τ_d whose origin still has to be ascertained. Both τ_d and R are q and $\dot{\gamma}$ dependent and respectively present a minimum and a maximum for a similar range of q . Other spinodal-like features of SID include the growth of domains of different compositions during an "intermediate stage" and spinodal-like patterns displayed by optical micrographs.

The minimal delay time τ_{dm} and the inverse of the maximal growth rate R_m decrease when shear rate increases and both present a sharp change in their behavior when $\dot{\gamma}$ approaches 1 s⁻¹. For a given shear rate, the global demixing process appears to be faster (i.e., higher R_m and lower τ_{dm} values) for blends with higher polydispersities and for lower experimental temperatures.

The SID process that we have shown to be highly temperature and shear rate (or stress) dependent, is also strongly influenced if the sample is in an initial non-equilibrium state either due to thermal or mechanical stress. For the present, none of these observations allow us to discriminate definitively between thermodynamic or hydrodynamic approaches to the problem of shear-induced demixing, each of these presenting reasonable explanations, at least qualitatively, for most of the observed features. The Clarke and McLeish approach nevertheless seems a promising one in a quantitative way for $\dot{\gamma}\tau < 1$.

Appendix

Theory of the Early Stages of Phase Separation.

To understand the early stage dynamics of phase separation following a "shear quench" at constant temperature, we can utilize the model of ref 40, which gives the equation of motion of concentration fluctuations in the vorticity \mathbf{z} direction, with $q_x = q_y = 0$, in the presence of shear as

$$\begin{aligned} \frac{\partial \delta \phi_A(\mathbf{q}, t)}{\partial t} &= q_z^2 \left[(D_{\text{app}0} - M\kappa q^2) - \frac{\alpha}{k_B T} \frac{\partial}{\partial \phi_A} \sigma_{zz}^{(n)}(t) \right] \delta \phi_A(\mathbf{q}, t) \\ &\equiv q_z^2 [(D_{\text{app}0} - M\kappa q^2) - \Delta D(t)] \delta \phi_A(\mathbf{q}, t) \quad (\text{A1}) \end{aligned}$$

where M , $D_{\text{app}0}$, and κ are defined in section IIb and $\alpha = ((\zeta_A'/\phi_A) - (\zeta_B'/\phi_B))/(\zeta_A' + \zeta_B')$, ζ_i' being the frictional drag per monomeric volume⁴¹ associated with component i . $\sigma_{zz}(n)$ is the only component of the network stress, due to the shear flow effects, which contributes to the equation of motion in the vorticity direction. Equation 1 is derived within the "adiabatic" approximation,⁵¹ which assumes that the local value of the network stress is directly coupled to the local concentration, and neglects any concentration dependence of the equation of motion for the stress itself.

The theory presented by Clarke and McLeish⁴⁰ assumed that the monomeric friction coefficients do not change with composition. For a blend such as PS/PVME, this assumption will not hold due to the strong compositional dependence of the glass transition temperature of the blend. This can be accounted for by a simple modification of the theory, which allows for the compositional dependence of the relaxation times, τ_A and τ_B . This leads to an extra term in the effective diffusion coefficient D_{eff} (analogous to the Cahn–Hilliard $-R(q)/q^2$) now given by

$$\begin{aligned} D_{\text{eff}}(\bar{q}_z) &= 2 M(\chi_0 - \chi + \kappa q_z^2) + \frac{4\alpha}{3k_B T} \mathbf{M} \dot{\gamma}^2 G_A \left\{ \tau_A^2 \left[\phi_A + \right. \right. \\ &\quad \left. \left. 4(1 - 2\phi_A) G^{1/2} \left(\frac{\tau'}{1 + \tau'} \right)^2 - (1 - \phi_A) G \tau^2 \right] + \right. \\ &\quad \left. \left(\phi_A^2 \tau_A \frac{\partial \tau_A}{\partial \phi_A} + 8\phi_A \phi_B G^{1/2} \left[\frac{\tau_A \tau_B}{(\tau_A + \tau_B)^3} \right] \left(\tau_B^2 \frac{\partial \tau_A}{\partial \phi_A} + \right. \right. \right. \\ &\quad \left. \left. \left. \tau_A^2 \frac{\partial \tau_B}{\partial \phi_A} \right) \right] + \phi_B^2 G \tau_B \frac{\partial \tau_B}{\partial \phi_A} \right\} \quad (\text{A2}) \end{aligned}$$

where \mathbf{M} is the mobility in unit volume ($\mathbf{M} = M^* v_m$, v_m being an average monomeric volume), χ is the Flory–Huggins interaction parameter, and χ_0 is its value on the spinodal. G_A and τ_A are the plateau shear modulus

and relaxation time of component A, and ϕ_A is its volumic fraction, $G' = G_B/G_A$, $\tau' = \tau_B/\tau_A$.

For a polymer solution or melt, at low enough shear rates, $\dot{\gamma}\tau < 1$, the network stress is minimally modeled by the Maxwell model,⁵² which gives the time dependence of σ_{zz} in terms of the first normal stress difference as

$$\sigma_{zz}^{(n)}(t) = -\frac{1}{3} N_1(t) = -\frac{1}{3} \int_{-\infty}^t \frac{\partial G(t-t')}{\partial t'} (t-t')^2 \dot{\gamma}^2(t') dt' \quad (\text{A3})$$

where $G(t-t')$ is the stress relaxation function, which for polymer blends depends on the dynamics and concentration of both components. If the double reptation concept^{53,54} is generalized to blends of chemically different polymers, and assuming stress relaxation for each component to be dominated by a single time scale, then⁴⁰

$$\begin{aligned} G(t-t') &= [\phi_A (G_A \exp\{-(t-t')/\tau_A\})^{1/2} + \\ &\quad \phi_B (G_B \exp\{-(t-t')/\tau_B\})^{1/2}]^2 \quad (\text{A4}) \end{aligned}$$

We take the strain rate to be imposed instantaneously at $t = 0$, such that

$$\begin{aligned} \dot{\gamma}(t) &= 0 \quad \text{for } t < 0 \\ \dot{\gamma}(t) &= \dot{\gamma} \quad \text{for } t > 0 \quad (\text{A5}) \end{aligned}$$

If we now assume the adiabatic approximation is also valid during the build up of stress, then the time dependence of the first normal stress difference is given by the following expression:

$$\begin{aligned} N_1(t) &= \dot{\gamma}^2 G_A [\phi_A^2 f_1(\tau_A, t) + 8\phi_A \phi_B G^{1/2} f_1(\tau_{AB}, t) + \\ &\quad \phi_B^2 G f_1(\tau_B, t)] \quad (\text{A6}) \end{aligned}$$

Here

$$\tau_{AB} = \frac{2\tau_A \tau_B}{\tau_A + \tau_B} \quad (\text{A7})$$

and

$$f_1(\tau, t) = \tau^2 - \left[\frac{1}{2} t^2 + \tau^2 + t\tau \right] \exp(-t/\tau) \quad (\text{A8})$$

Hence, ΔD grows from zero at $t = 0$ to its final steady-state value, which may be positive or negative.⁴⁰ Once a steady state has been reached

$$\begin{aligned} N_1 &= 2\dot{\gamma}^2 \tau_A^2 G_A \left[\phi_A^2 + 8\phi_A \phi_B G^{1/2} \left(\frac{\tau'}{(1 + \tau')^2} \right)^2 + \right. \\ &\quad \left. \phi_B^2 G \tau'^2 \right] \quad (\text{A9}) \end{aligned}$$

and the effective diffusion coefficient is given by eq A2. If the composition dependence of the monomeric friction coefficient is neglected, the effective diffusion coefficient is given by eq 15 of ref 40. Previously, theoretical work has focused on behavior in the steady state. While such an approach is instructive in determining whether concentration fluctuations will be stable or unstable, it does not help us to understand the dynamics of phase separation after the imposition of shear. From eq A1, we may determine the scattering function, $S(q_z, t)$, if we

neglect the effects of noise, as

$$S(q_z t) = \langle |\delta\phi_A(q_z t)|^2 \rangle = S(q_z t = 0) \exp\{2q_z^2[(D_{\text{app}0} - M\kappa q_z^2)t - \int_0^t \Delta D(t')_c dt']\} \quad (\text{A10})$$

The experiments are carried out within the quiescent miscible region of the phase diagram; hence, without shear, concentration fluctuations decay with time. The experiments reported here show that, after the imposition of shear, phase separation takes place after some delay time. As discussed in the main text, the fact that phase separation occurs implies that ΔD is negative. Once this condition has been established, the most obvious interpretation of the delay time is that it is the time necessary for the magnitude of $\Delta D(t)$ to be significant enough to overcome the quiescent effects, which drive mixing. It is only when this occurs that $R(q_z)$ will become positive, so that fluctuations grow rather than decay. A complete analysis of eq A8 is not possible without detailed knowledge of the rheological parameters, τ_A , τ_B , G_A , and G_B . To gain a crude approximation to the time dependence, we shall assume that τ_A and τ_B are of the same order of magnitude (which is indeed more than unlikely for PS/PVME), and that the concentration dependence of each is similar, which gives $\Delta D(t)$ as

$$\Delta D(t) \approx \frac{4\alpha M}{3k_B T} \dot{\gamma}^2 G_A \left\{ \tau_A^2 [\phi_A + (1 - 2\phi_A)G^{1/2} - (1 - \phi_A)G] f_1(1, x) + \tau_A \frac{\partial \tau_A}{\partial \phi_A} [\phi_A^2 + \phi_A(1 - \phi_A)G^{1/2} + (1 - \phi_A^2)G] f_2(1, x) \right\} \quad (\text{A11})$$

where

$$x = t/\tau_{AB} \approx t/\tau_A \approx t/\tau_B \quad (\text{A12})$$

and

$$f_2(\tau, t) = \left(2\tau \frac{\partial \tau}{\partial \phi_A}\right)^{-1} \frac{\partial f_1}{\partial \phi_A} = 1 - \left[1 + \frac{t}{\tau} + \frac{t^2}{2\tau^2} + \frac{t^3}{4\tau^3}\right] \exp\{-t/\tau\} \quad (\text{A13})$$

As already stated in the Discussion, we cannot yet ascertain the relative significance of the two contributions (the one involving f_1 and the one involving f_2 taking into account the composition dependence of relaxation time). Hence, we will examine the consequences of each term on an expected delay time. Neglecting the second term on the right-hand side of eq A11, i.e., the term proportional to f_2 , allows us to predict a relationship between the expected "reduced" delay time, x_{d1} , and the observed final growth rate

$$f_1(1, x_{d1}) \approx \left| \frac{D_{\text{app}0}}{A\dot{\gamma}^2} \right| \quad (\text{A14})$$

Now, if we consider the f_2 term to be more significant, we can now predict a second 'reduced' delay time, x_{d2} with

$$f_2(1, x_{d2}) \approx \left| \frac{D_{\text{app}0}}{A\dot{\gamma}^2} \right| \quad (\text{A15})$$

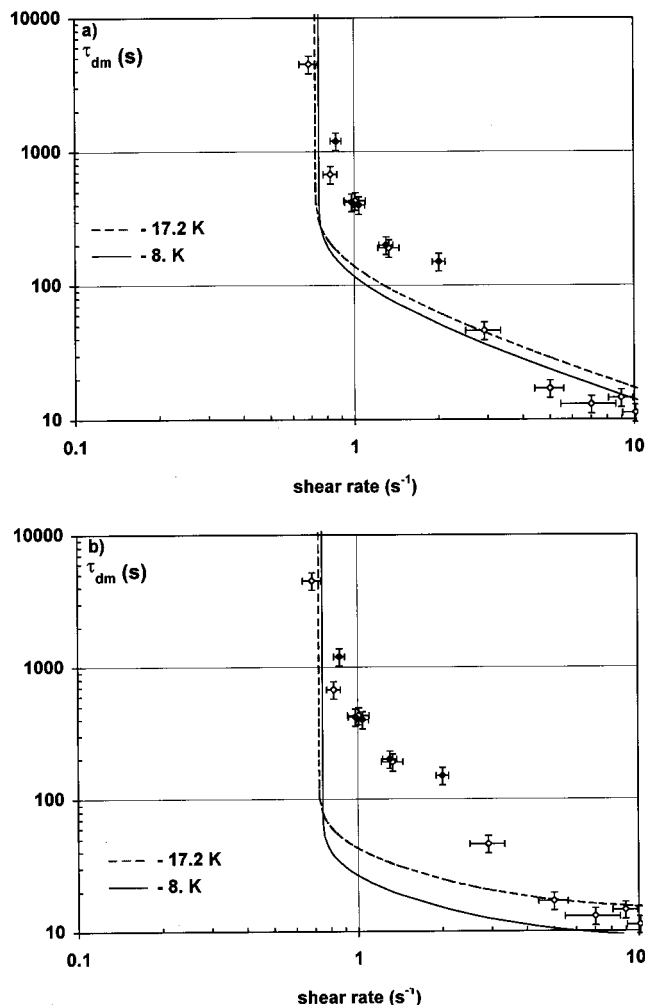


Figure 12. Delay time as a function of shear rate: experimental data for blend 1 at $\Delta T = -17.2$ K (open symbols) and -8 K (filled symbols) and as determined using (a) eq A14 with $\tau_{AB} = 50$ s (-17.2 K) and $\tau_{AB} = 40$ s (-8 K) and (b) eq A15 with $\tau_{AB} = 10$ s (-17.2 K) and $\tau_{AB} = 6$ s (-8 K).

The two terms on the right-hand side are given in Table 2, and eqs A14 and A15 may then be solved to find x_{d1} and x_{d2} as a function of shear rate. While the x_{d1} leads to a reasonable agreement with regards to the shear rate dependence of the delay time (see Figure 12), it leads to molecular relaxation times orders of magnitude greater than would be expected for such blends.⁵⁵ The x_{d2} values present a stiffer behavior but require smaller relaxation times to fit the values found for experimental delay times.

This early attempt to describe the observed delay time as the time needed to develop a sufficient shear stress to observe SID after a shear jump seems to fail. It is surely too simplistic, since the assumption $\tau_A \approx \tau_B$ is unlikely to be verified for our system (need to use three characteristic relaxation times to express $N_1(t)$ as in eq A6) and the f_1 and f_2 terms are likely to both contribute to the phenomenon. Moreover, the polydispersity of the system has not been taken into account and will strongly affect the time behavior of the shear stress, possibly adding a distribution of relaxation times for each component.

Acknowledgment. The authors would like to thank Prof. R. A. Weiss, Dr. S. Mani (University of Connecticut), Prof. T. Hashimoto and Dr. T. Kume (Uni-

versity of Kyoto) for their invaluable help and advice during early experiments, Prof. T. C. B. McLeish (University of Leeds, IRC), Prof. S. Ross-Murphy (King's College, London) for early rheological experiments, and Dr. V. M. C. Reid and N. J. J. Aelmans (DSM Research) for the work they enabled us to carry out at DSM. This work was supported by the EU (Brite/Euram Grant BRE2-CT94-0610).

References and Notes

- (1) Hindawi, I. A.; Higgins, J. S.; Weiss, R. A. *Polymer* **1992**, *33*, 2522.
- (2) Mazich, K. A.; Carr, S. H. *J. Appl. Phys.* **1983**, *54*, 5511.
- (3) Katsaros, J. D.; Malone, M. F.; Winter, H. H. *Polym. Bull.* **1986**, *16*, 83.
- (4) Lyngaae-Jorgensen, J.; Sondergaard, K. *Polym. Eng. Sci.* **1987**, *27*, 351.
- (5) Nakatani, A. I.; Kim, H.; Takahashi, H.; Matsushita, Y.; Takano, A.; Bauer, B. J.; Han, C. C. *J. Chem. Phys.* **1990**, *93*, 795.
- (6) Kim, S.; Hobbie, E. K.; Yu, J. W.; Han, C. C. *Macromolecules* **1997**, *30*, 8245.
- (7) Fernandez, M. L.; Higgins, J. S.; Richardson, S. M. *Trans. Inst. Chem. Eng.* **1993**, *71A*, 293.
- (8) Katsaros, J. D.; Malone, M. F.; Winter, H. H. *Polym. Eng. Sci.* **1989**, *29*, 1434.
- (9) Mani, S.; Malone, M. F.; Winter, H. H. *Macromolecules* **1992**, *25*, 5671.
- (10) Werner, D. E.; Fuller, G. G.; Frank, C. W. In *Theoretical and Applied Rheology (Proceedings of the XIth International Congress on Rheology)*; Moldenaers, P., Keunings, R., Eds.; Elsevier: Amsterdam, 1992; p 402.
- (11) Fernandez, M. L.; Higgins, J. S.; Horst, R.; Wolf, B. A. *Polymer* **1995**, *36*, 149.
- (12) Hindawi, I.; Higgins, J. S.; Galambos, A. F.; Weiss, R. A. *Macromolecules* **1990**, *23*, 670.
- (13) Fernandez, M. L.; Higgins, J. S.; Richardson, S. M. *J. Mater. Process. Technol.* **1996**, *56*, 807.
- (14) Aelmans, N. J. J.; Reid, V. M. C.; Higgins, J. S. *Polymer* **1999**, *40*, 5051.
- (15) Chopra, D.; Vlassopoulos, D.; Hatzikiriakos, S. G. *J. Rheol.* **1998**.
- (16) (a) Bank, M.; Leffingwell, J.; Thies, C. J. *J. Polym. Sci., Polym. Phys. Ed.* **1972**, *10*, 1097. (b) Kwei, T. K.; Nishi, T.; Roberts, R. F. *Macromolecules* **1974**, *7*, 667. (c) Urbrish, J. M.; Ben Cheikh Larbi, F.; Halary, J. L.; Monnerie, L.; Bauer, B. J.; Han, C. C. *Macromolecules* **1986**, *19*, 810.
- (17) Horst, R.; Wolf, B. A. *Macromolecules* **1993**, *26*, 5676.
- (18) Cahn, J. W. *Trans. Met. Soc. AIME* **1968**, *242*, 169.
- (19) Cahn, J. W.; Hilliard, J. E. *J. Chem. Phys.* **1958**, *28*, 258.
- (20) Hashimoto, T. *Phase Transitions* **1988**, *12*, 47.
- (21) de Gennes, P.-G. *J. Chem. Phys.* **1980**, *72*, 4756.
- (22) Clarke, N.; McLeish, T. C. B.; Pavawongsak, S.; Higgins, J. S. *Macromolecules* **1997**, *30*, 4459.
- (23) Onuki, A.; Taniguchi, T. *J. Chem. Phys.* **1997**, *106*, 5671.
- (24) Sato, T.; Han, C. C. *J. Chem. Phys.* **1988**, *88*, 2057.
- (25) Pistor, N.; Binder, K. *Colloid Polym. Sci.* **1988**, *266*, 132.
- (26) Ji, H.; Helfand, E. *Macromolecules* **1995**, *28*, 3869.
- (27) Larson, R. G. *Rheol. Acta* **1992**, *31*, 497.
- (28) Milner, S. T. *Phys. Rev. E* **1993**, *48*, 3674.
- (29) Onuki, A.; Yamamoto, R.; Taniguchi, T. *J. Phys. II Fr.* **1997**, *7*, 295.
- (30) Marrucci, G. *Trans. Soc. Rheol.* **1972**, *16*, 321.
- (31) Horst, R.; Wolf, B. A. *Macromolecules* **1992**, *25*, 5291.
- (32) Rangel-Nafaile, C.; Metzner, A.; Wissburn, K. *Macromolecules* **1984**, *17*, 1187.
- (33) Wolf, B. A. *Macromolecules* **1984**, *17*, 615.
- (34) Soontaranun, W.; Higgins, J. S.; Papathanasiou, T. D. *Fluid Phase Equilibria* **1996**, *121*, 273.
- (35) Chopra, D.; Haynes, C.; Hatzikiriakos, S. G.; Vlassopoulos, D. *J. of Non-Newtonian Fluid Mech.* **1999**, *82*, 367.
- (36) Onuki, A. *J. Phys. Condens. Matter* **1997**, *9*, 6119.
- (37) Brochard, F.; de Gennes, P.-G. *Macromolecules* **1977**, *10*, 1157.
- (38) Doi, M.; Edwards, S. F. In *The Theory of Polymer Dynamics*; Clarendon Press: Oxford, U.K., 1986.
- (39) Hashimoto, T.; Kume, T. *J. Phys. Soc. Jpn* **1992**, *61*, 1839.
- (40) Clarke, N.; McLeish, T. C. B. *Phys. Rev. E* **1998**, *57*, R3731.
- (41) Doi, M.; Onuki, A. *J. Phys. II Fr.* **1992**, *2*, 1631.
- (42) Kapnistos, M.; Hinrichs, A.; Vlassopoulos, D.; Anastasiadis, S. H.; Stammer, A.; Wolf, B. A. *Macromolecules* **1996**, *29*, 7155.
- (43) Ferry, J. D. In *Viscoelastic Properties of Polymers*, 3rd ed.; Wiley: New York, 1980.
- (44) Chen, Z. J.; Shaw, M. T.; Weiss, R. A. *Macromolecules* **1995**, *28*, 648.
- (45) Fernandez, M. L.; Higgins, J. S.; Richardson, S. M. *Polymer* **1995**, *36*, 931.
- (46) Remediakis, N. G.; Weiss, R. A.; Shaw, M. T. *Rubber Chem. Technol.* **1997**, *70*, 71.
- (47) Taylor, G. I. *Proc. R. Soc. London* **1934**, *A146*, 501.
- (48) Elmendorp, J. J.; van der Vegt, A. K. *Polym. Eng. Sci.* **1986**, *26*, 1332.
- (49) Sundararaj, U.; Macosko, C. W. *Macromolecules* **1995**, *28*, 2647.
- (50) Fukuda, T.; Fujimoto, K.; Tsujii, Y.; Miyamoto, T. *Macromolecules* **1996**, *29*, 3300.
- (51) Milner, S. T. *Phys. Rev. E* **1993**, *48*, 3674.
- (52) Larson, R. G. *Constitutive Equations for Polymer Melts and Solutions*; Butterworths: Boston, MA, 1988.
- (53) des Cloizeaux, J. *Europhysics Lett.* **1988**, *5*, 437.
- (54) Tsenoglu, C. *Macromolecules* **1991**, *24*, 1762.
- (55) Pathak, J. A.; Colby, R. H.; Floudas, G.; Jérôme, R. *Macromolecules* **1999**, *32*, 2553.

MA981635+